



Radiation effects on RPV and internals microstructure

Mechanisms of formation of nano-features in RPV (steels and model alloys)

Contributions from CEA, CIEMAT, CVR, HZDR and CNRS

DE LA RECHERCHE À L'INDUSTRIE



www.cea.fr

Contribution from CEA:

Study of RPV model material (FeMn and FeNi model alloys)

Estelle MESLIN – CEA/SRMP

PhD of Lisa BELKACEMI (2015-2018) -CEA/SRMP

Brigitte DECAMPS – CSNSM – CNRS

Maylise NASTAR – CEA/SRMP

Marie LOYER-PROST - CEA/JANNUS

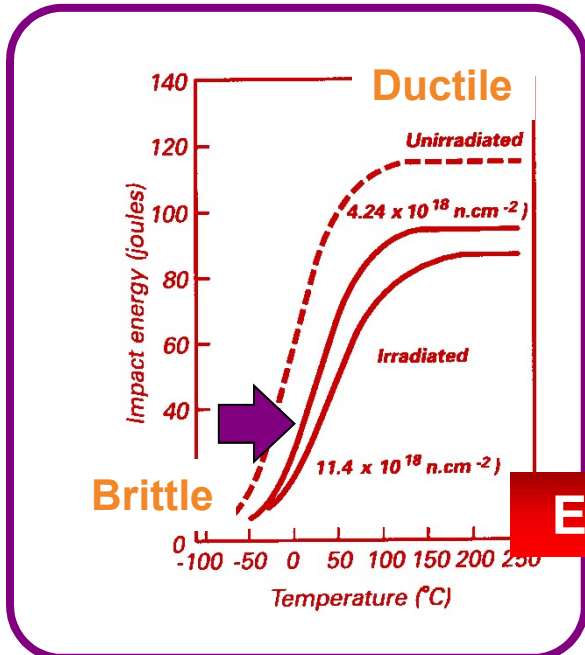
Jean HENRY – CEA/SRMA

Bertrand RADIGUET – GPM – CNRS

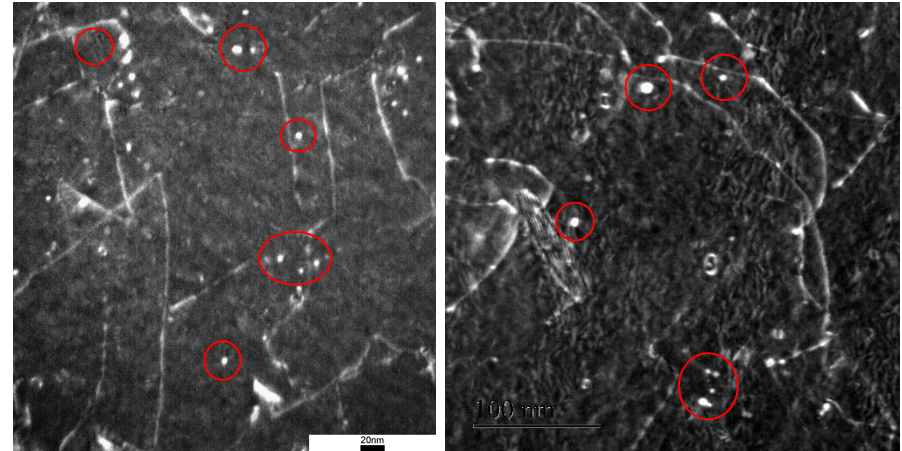
RPV STEEL EMBRITTLEMENT UNDER IRRADIATION

Reactor Pressure Vessel (RPV) Steel:

Fe – **Cu**, Mn, Ni, C, P, N, S, Si, Mo, Al, Cr

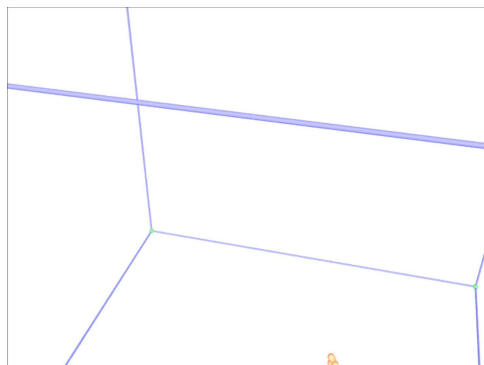


RPV steel (16MND5), surveillance flux (10^{-10} dpa/s)
neutron, 155 bar, End of Life = 0.1 dpa, 300° C



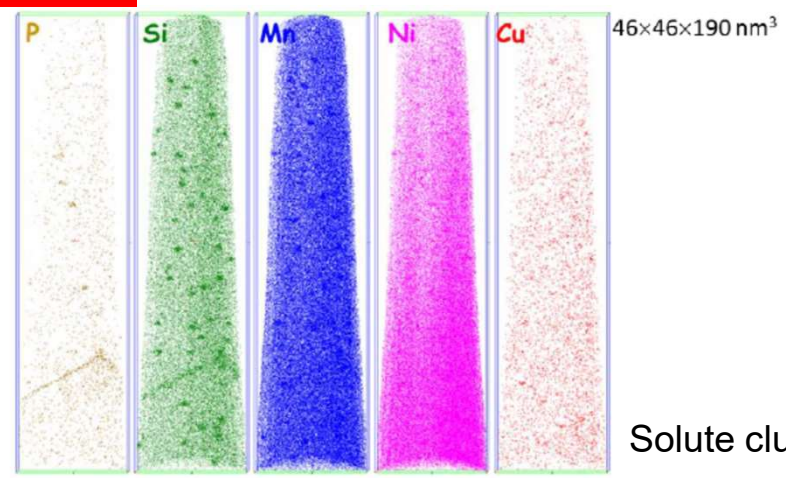
CEA Saclay, WBDF TEM Point Defect clusters

Embrittling clusters



MD: 500 keV Fe
ions Fe in Fe

Acknowledgements
to Cosmin Mihai
Marinica



Solute clusters

GPM Rouen, APT

SIMPLIFICATION OF IRRADIATION CONDITIONS AND MATERIALS

Experiments

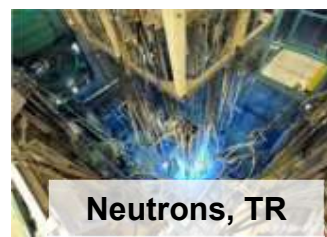
Ions/neutrons representativity



Damage rate

10^{-5} - 10^{-3} dpa/s

Flux effect ?



Neutrons, TR

10^{-9} - 10^{-7} dpa/s



Neutrons, RPV

10^{-10} dpa/s

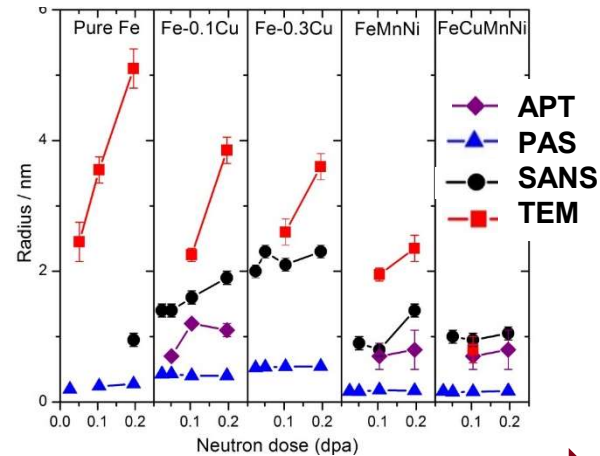
Operation

Rationalisation of neutron irradiation campaign

Simulation of real materials: model materials

Example of Cu, Mn and Ni in FeCu, FeMnNi and FeCuMnNi alloys

Neutrons, Test Reactor



Increase of alloy complexity

Perfect project, JNM, 406, 73-83 (2010)

CLUSTERS OF DEFECTS' CONTRIBUTION TO THE EMBRITTLEMENT

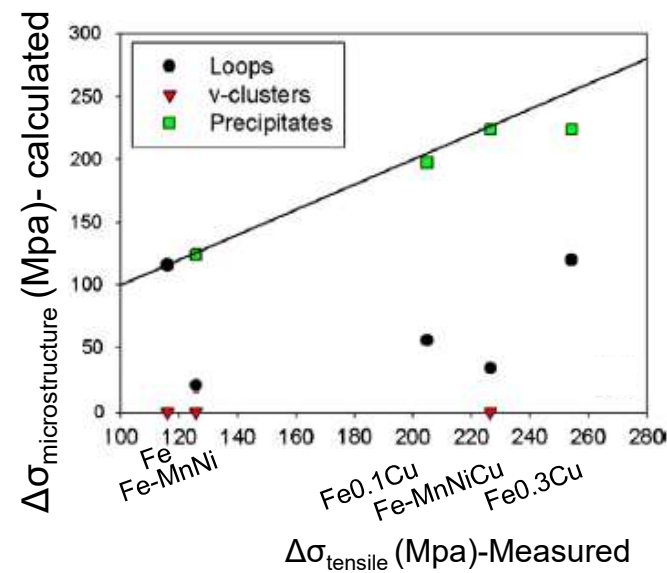
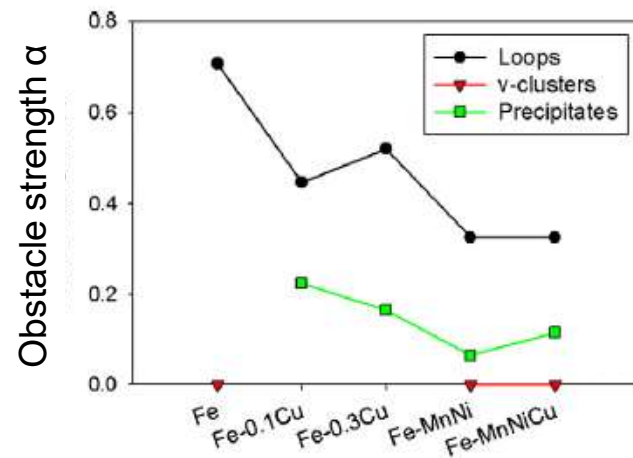
[Perfect project, JNM 406, pp. 84-89 (2010)]

- Orowan equation to calculate the clusters of defects' contribution to the embrittlement:

$$\Delta\sigma = \alpha \cdot M \cdot G \cdot b \cdot \sqrt{N \cdot d}$$



α : Obstacle strength
M: Taylor factor: 3.06
G: Shear modulus



Dislocation loops: Highest obstacle strength but low density

Cavities: Numerous but very low obstacle strength

Solute clusters: High contribution to the embrittlement (high density)

Associated to small PD clusters (Invisible PD clusters or cavities?)

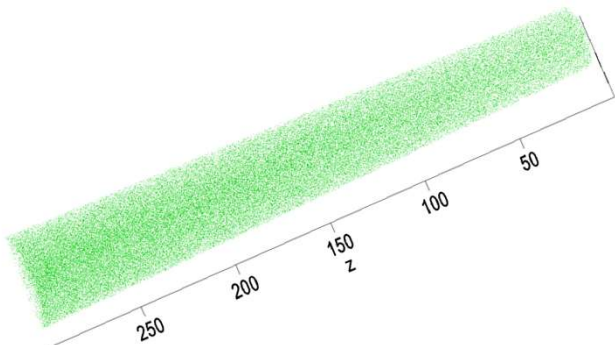
Necessity to study the position correlation between solute clusters and PD clusters

Model ferritic materials : Fe-3%Ni et Fe-3%Mn

Parametrized Ion irradiation (flux effects)

Combined nano-characterization techniques

Model alloy: Fe3%Ni



Non irradiated Fe3%Ni alloy

Ni homogeneously distributed within the volume

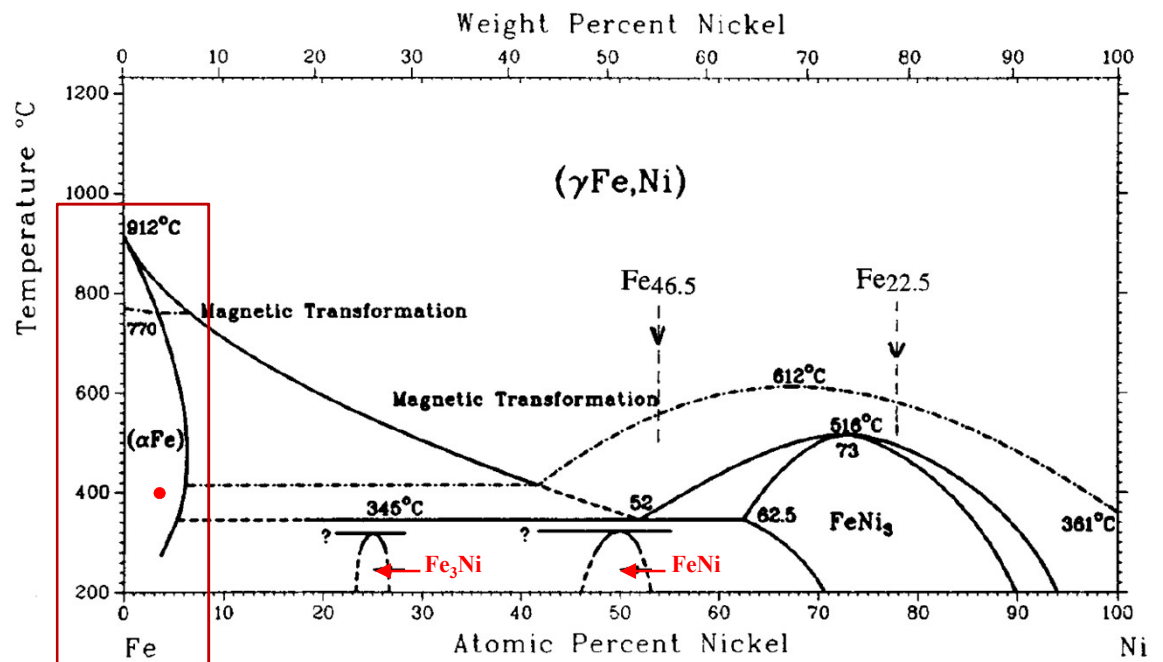
Solubility limit @ 673 K : ~ 6 at.%

Fully ferritic material

Single phase

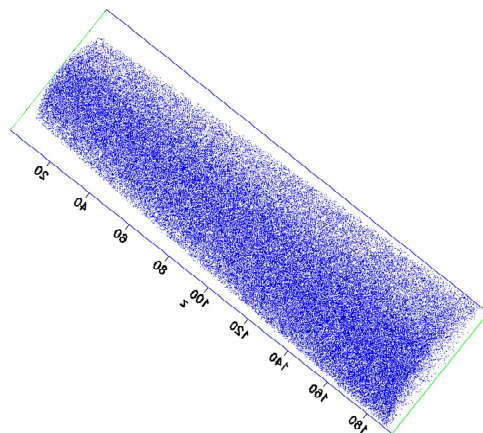
High purity material (EMSE)

Element	Ni (at.%)	C (appm)	S (appm)	O (appm)	N (appm)
Fe3%Ni	3.2	23	4	35	4



Binary Alloy Phase Diagrams American Society for Metals, Metals Park, CA, 1986, Vol. 1.

Model alloy: Fe3%Mn



Non irradiated Fe3%Mn

Homogeneous Mn repartition

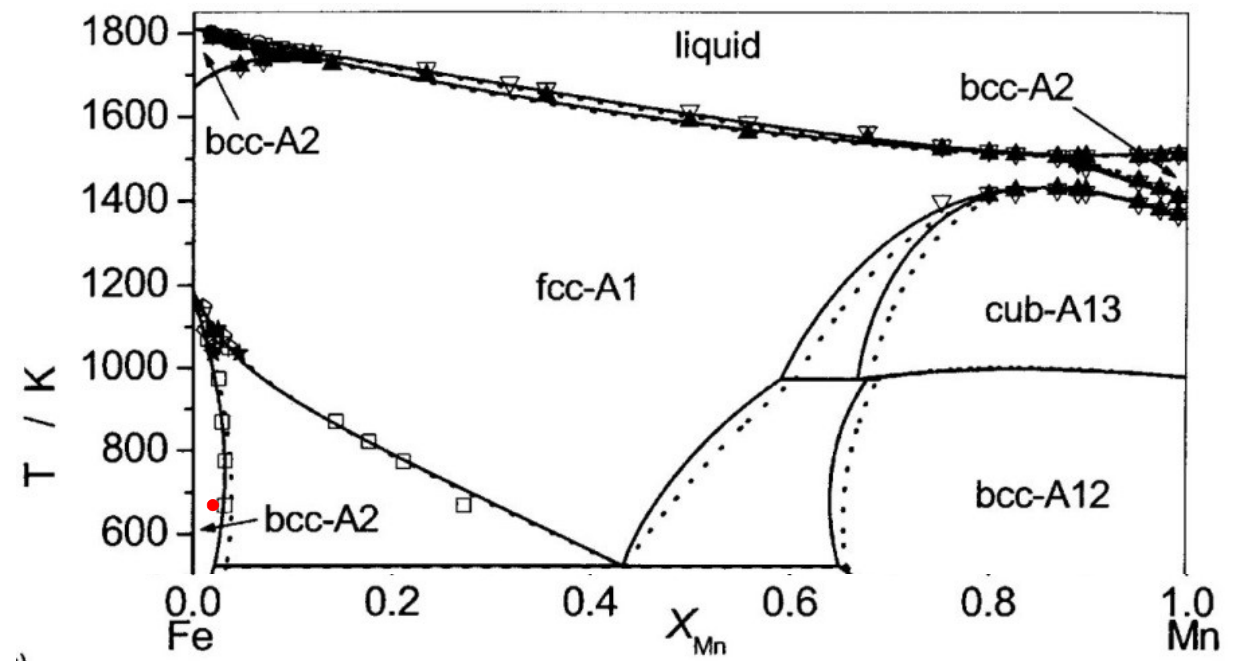
Solubility limit @ 400° C (673 K) :
~ 6 at.%

Fully ferritic

→ Single phase

High purity (EMSE)

Eléments	Mn (at.%)	C (appm)	S (appm)	O (appm)	N (appm)
Fe3%Mn	2.85	21	14	3	5



Ion irradiation: Flux effect

- Ions Fe
- 673K
- 1.2 dpa

x 65

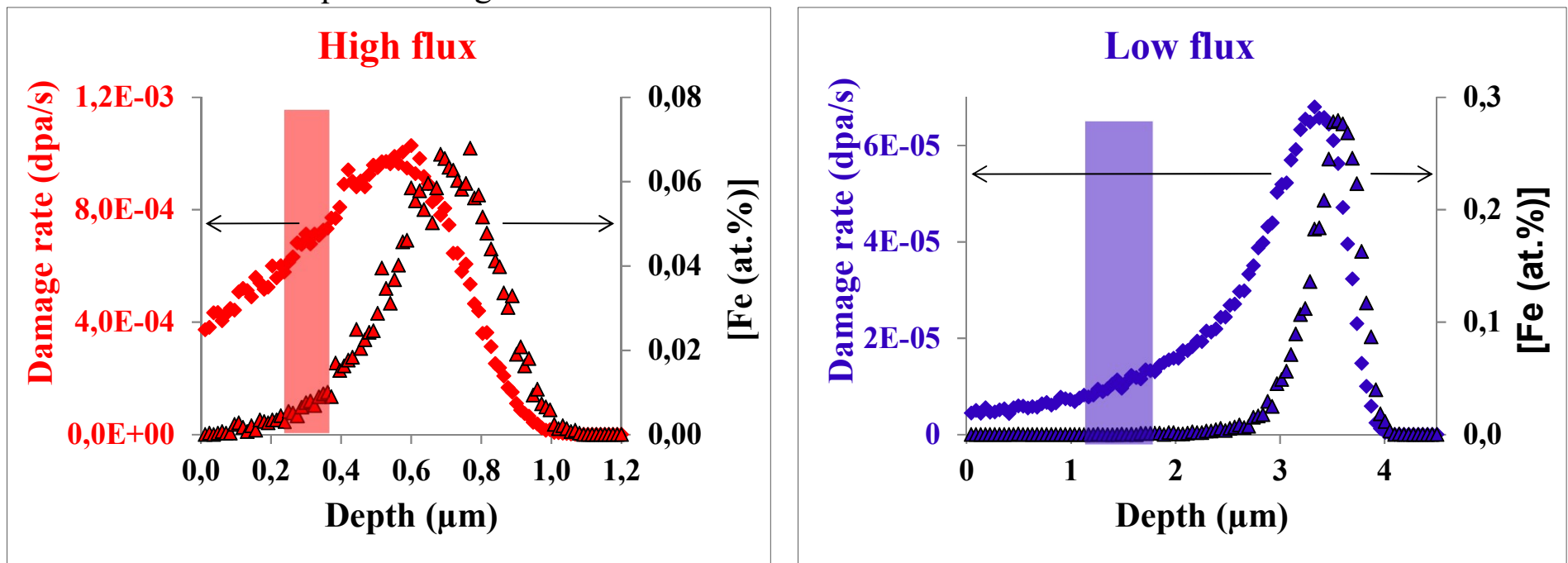
SRIM calculation « quick damage »

- 2 damage rates:

- 27 MeV Fe^{9+} ions, $8.7 \times 10^{10} \text{ ions.cm}^{-2}.\text{s}^{-1}$
 $1.4 \times 10^{16} \text{ ions.cm}^{-2}$, **$8 \times 10^{-6} \text{ dpa.s}^{-1}$**
- Fe^{3+} de 2 MeV, $8.6 \times 10^{11} \text{ ions.cm}^{-2}.\text{s}^{-1}$
 $2.1 \times 10^{15} \text{ ions.cm}^{-2}$, **$5.2 \times 10^{-4} \text{ dpa.s}^{-1}$**



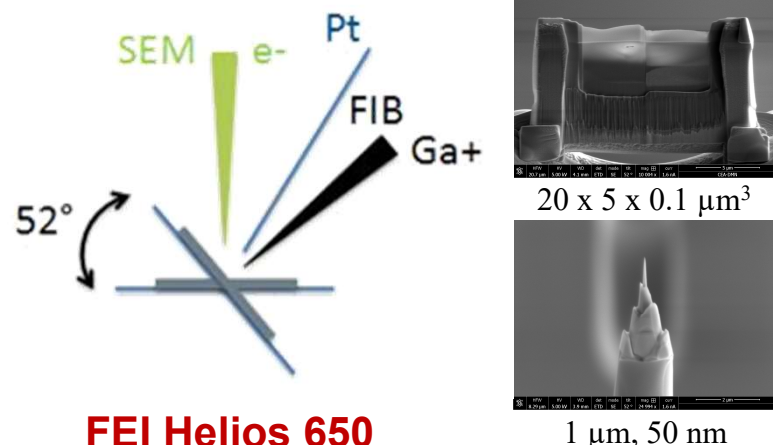
Acknowledgements at
JANNuS-Saclay



1 dose ; 2 damage rates

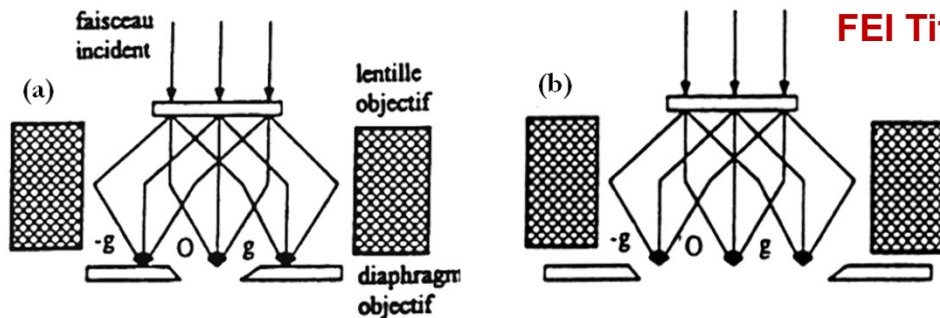
Nano-characterization techniques

FIB : Sample preparation

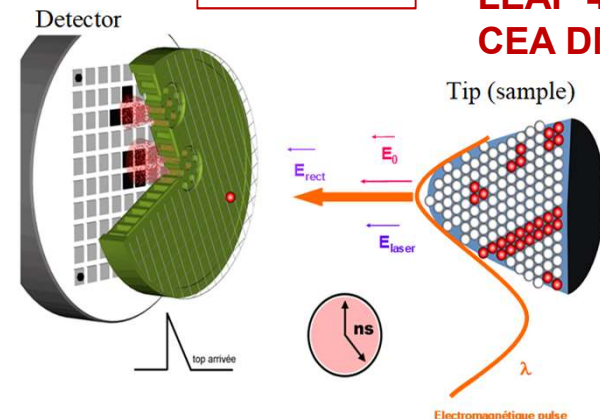


Conventional TEM and HR

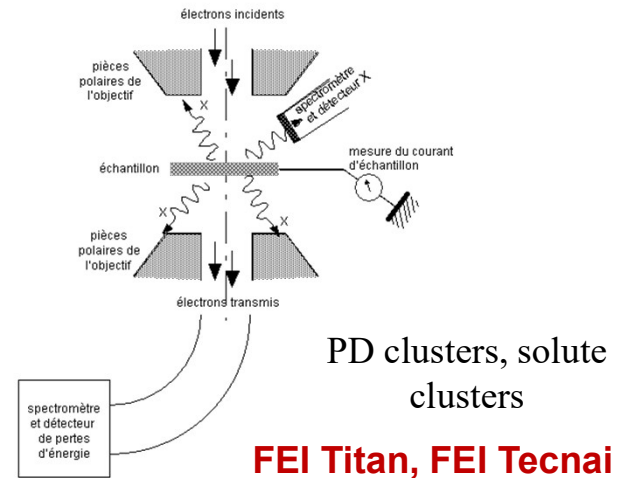
Dislocation loops (I ou L), cavities, precipitates



APT



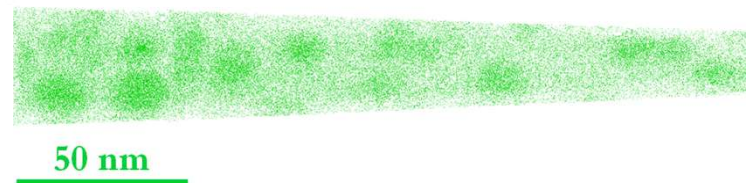
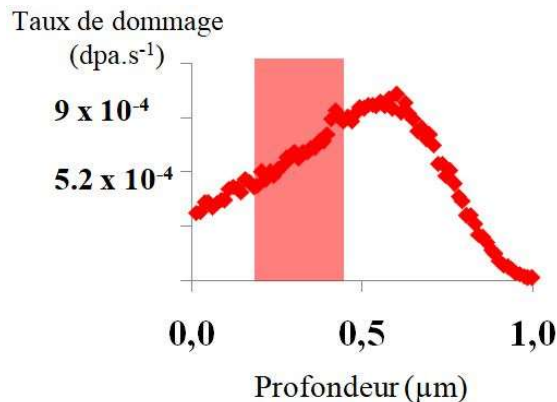
STEM/EDS, STEM/EELS



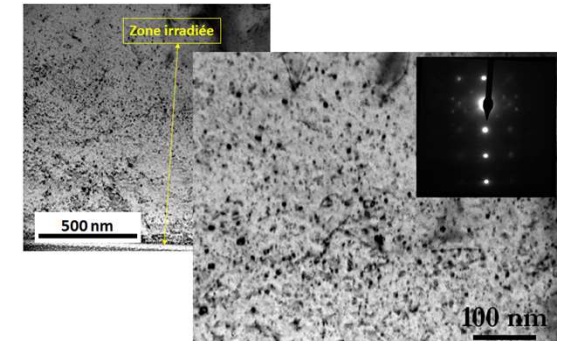
Correlation between structural and chemical informations

Flux effect in Fe3%Ni alloy

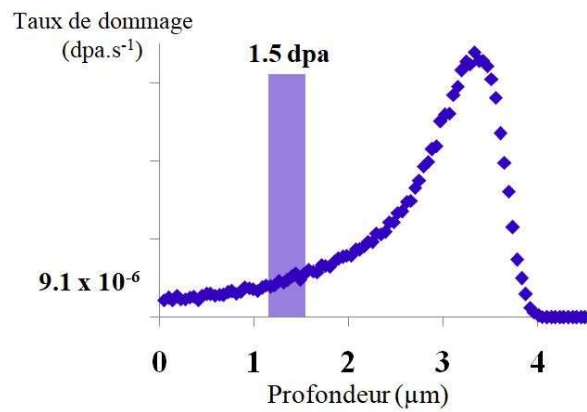
High flux



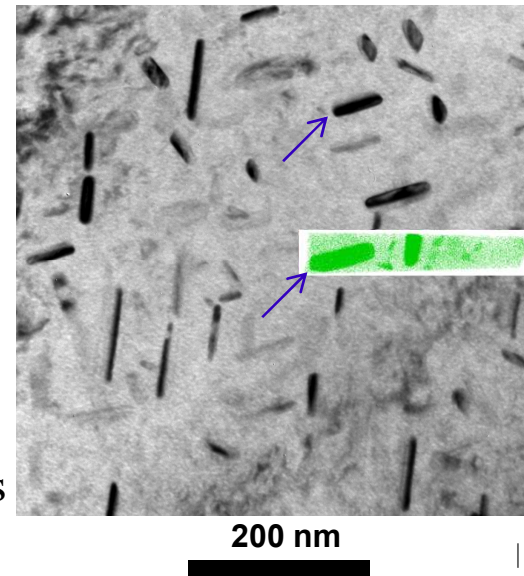
Spherical Ni clusters segregated on
dislocation loops
 17.0 ± 0.3 at.% Ni



Low flux

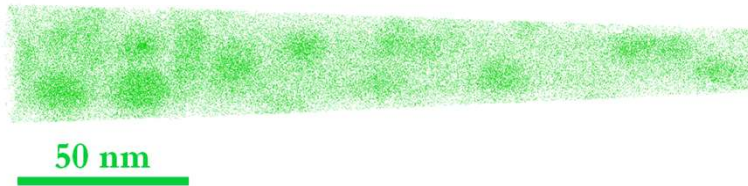


FCC precipitates
 ~ 25 at.% Ni



Flux effect in Fe3%Ni alloy

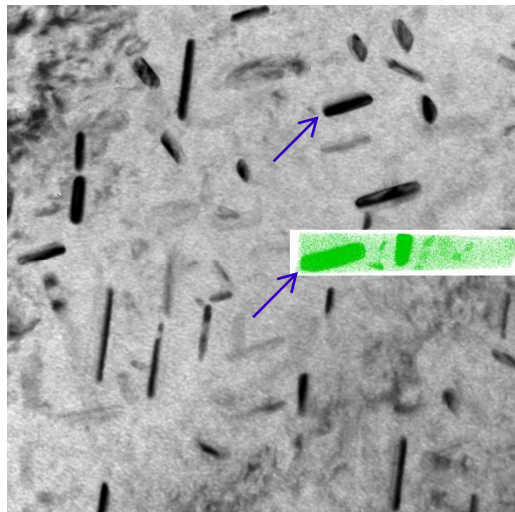
High flux



Radiation-induced segregation (RIS)

- Segregated atomic fraction: 5.2 %

Low flux

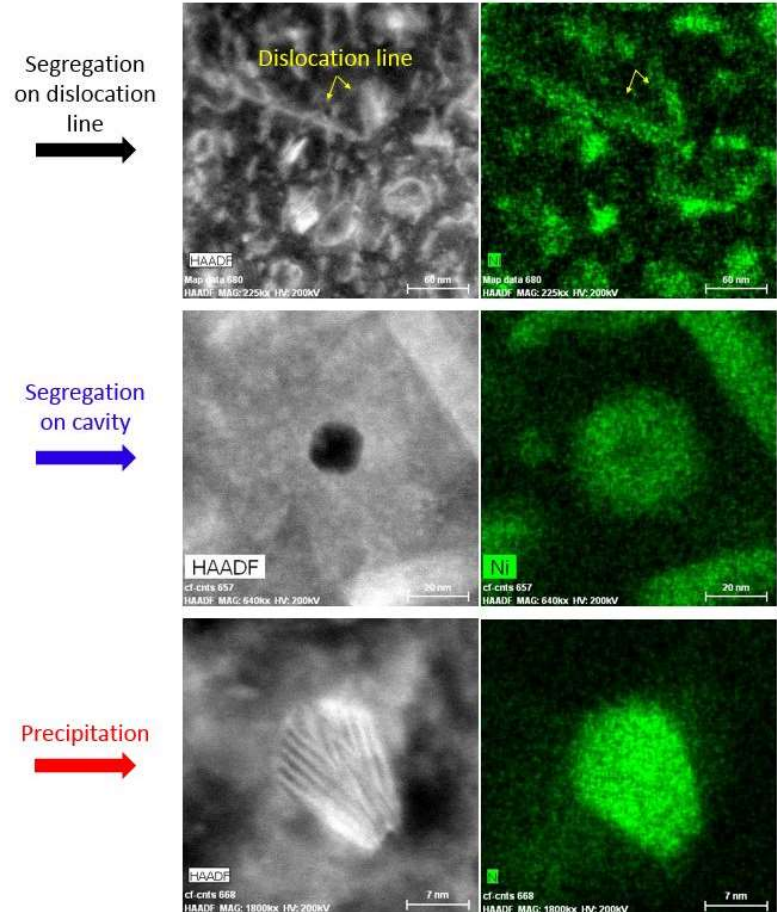
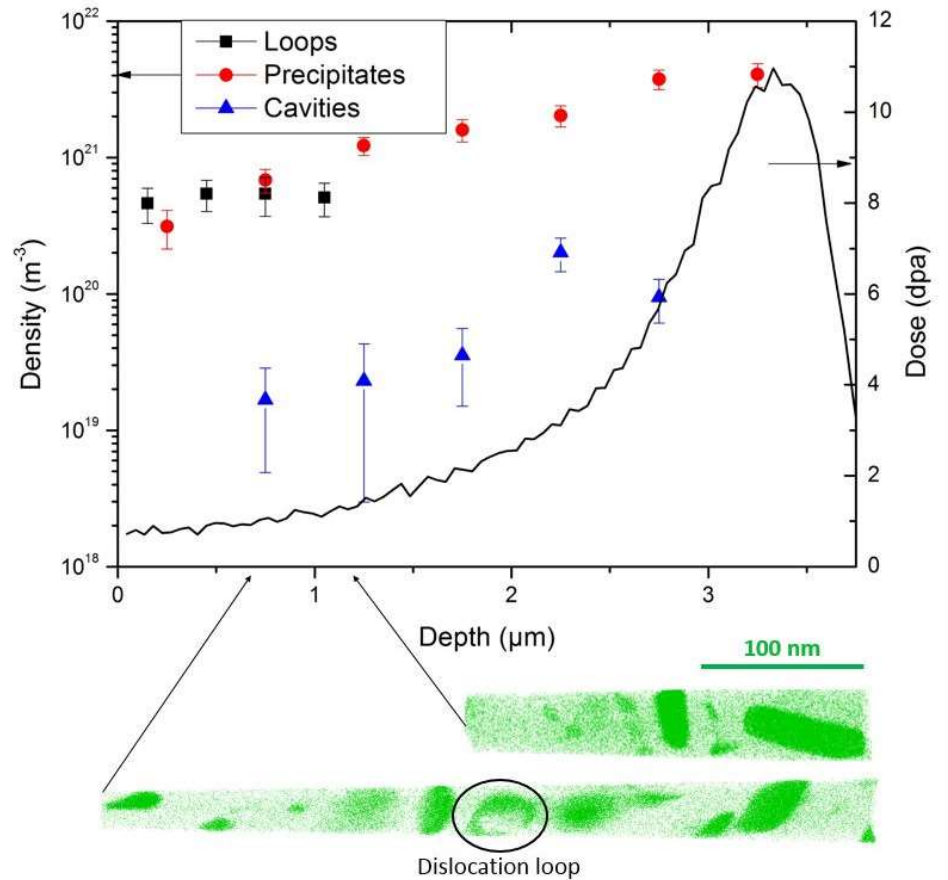


Radiation-induced precipitation (RIP)

- FCC precipitates: ~ 25 at.% Ni
- Disordered Fe-25%Ni or L₁₂ type intermetallic Fe₃Ni precipitates
- Precipitated atomic fraction: 66.2 %

High flux effect on the kinetics of Ni precipitation

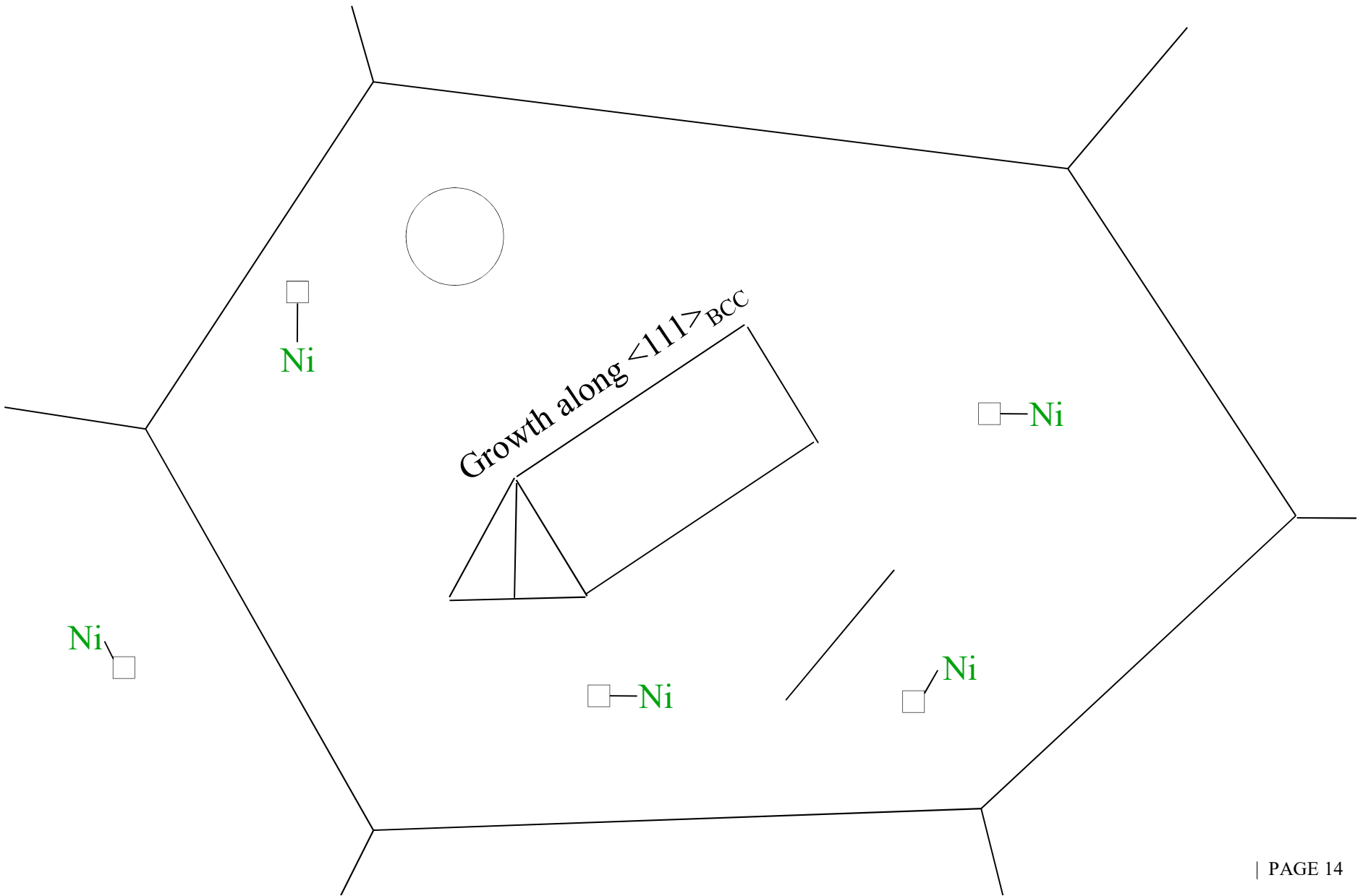
Low flux: Radiation-induced bcc-fcc phase transformation



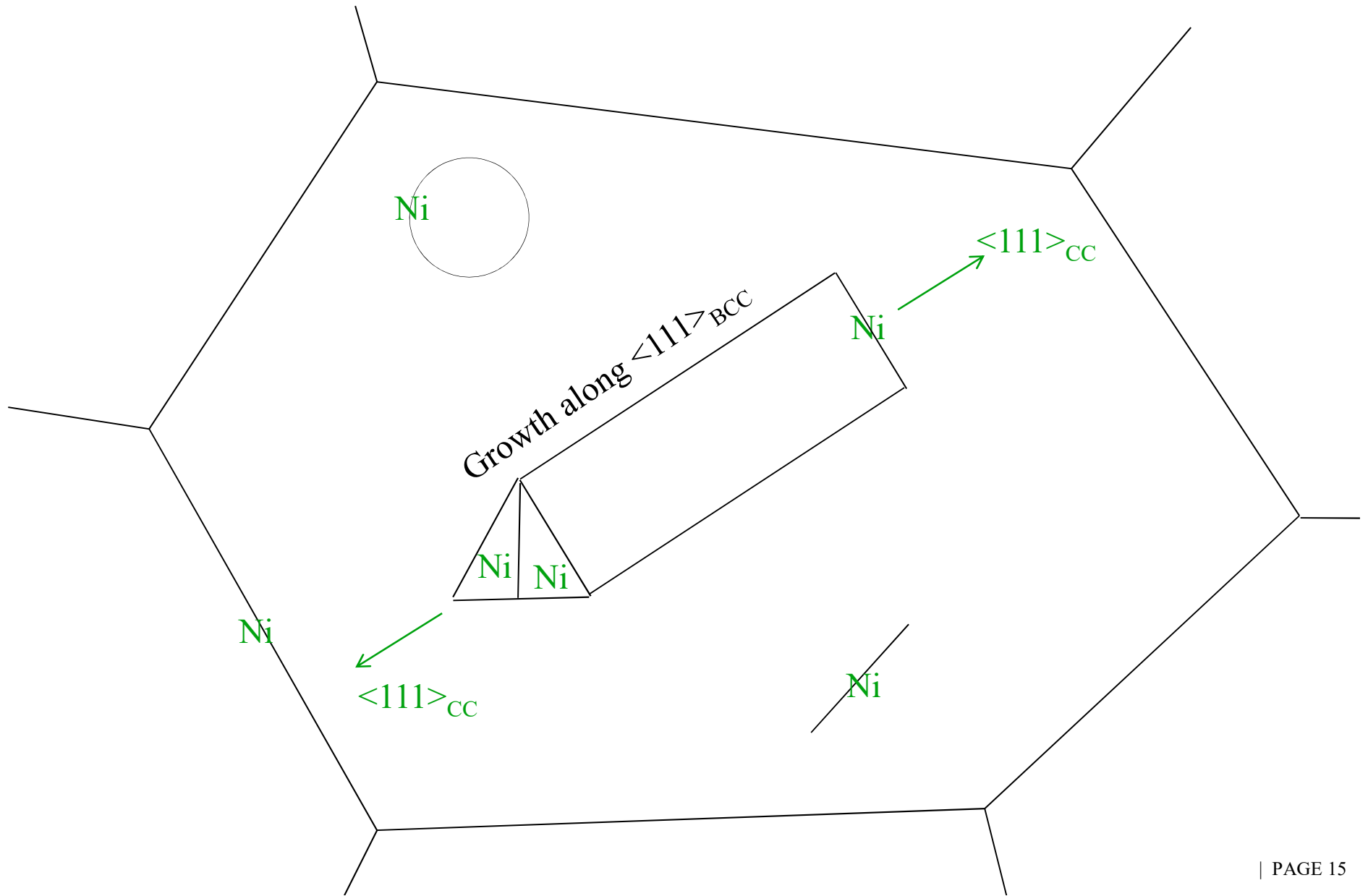
L. T. Belkacemi et al., Acta Materialia, 161, 2018, 61-72

FCC - BCC interface = PD sinks

Low flux: Radiation-induced bcc-fcc phase transformation



Low flux: Radiation-induced bcc-fcc phase transformation



Comparison between Mn and Ni

2.1 dpa
TEM analyses (dislocation loops)

		High flux	Low flux
Fe3%Ni	Diameter(nm)	2.8 ± 1	47.9
	Density(m^{-3})	2.6×10^{22}	$1.6 \pm 0.3 \times 10^{21}$
Fe3%Mn	Diameter (nm)	10.9 ± 3	$<111> : 41 \pm 6$ $<100> : 81 \pm 26$
	Density (m^{-3})	$> 10^{23}$	5.9×10^{20}

Different behavior

Comparison between Mn and Ni

APT analyses

	High flux	Low flux
Solute content(%at.)	17.0	~ 25
Fe3%Ni		
Atomic fraction seg/pre(%)	5.2	66.2
Solute content (%at.)	$26.7 < \text{Mn} < 38.5$	→ 56.8
Fe3%Mn		
Atomic fraction seg/pre(%)	9.5	-

Highest tendency of Mn to precipitate

CONCLUSIONS

- Fe3%Ni:

High flux : Radiation induced segregation

Low flux : Radiation induced precipitation:

γ precipitates aligned along <111> direction of the BCC matrix

Kurdjumov-Sachs relationship

Growth at FCC/BCC interface (= PD sinks)

- Fe3%Mn:

High and low flux: Radiation induced segregation (precipitation ?)

- Flux coupling:

Mn: more efficient dragging through vacancy and SIA than Ni → enrichment more important at PD sinks

Contribution from HZDR

Nanoindentation data obtained on ion-irradiated RPV steels

[F. Röder, C. Heintze, S. Pecko, S. Akhmadaliev, F. Bergner, A. Ulbricht, and E. Altstadt, *Nanoindentation of ion-irradiated reactor pressure vessel steels – model-based interpretation and comparison with neutron irradiation*, Phil. Mag. 98 (2018), pp. 911–933]

Composition studied

Material	Code	Product	Final heat treatment	Manufacturer	σ_v (MPa)
A508 cl. 3	JFL	forging	880 °C/9h, w.c., 640° C/9h, a.c.	Kawasaki Steel Corp., Japan	470
A533B cl. 1 model steels	JPB	plate	880° C/1h, a.c., 670° C/80min, a.c.	Nippon Steel Corp., Japan	511
A533B cl. 1	JRQ	plate	880°C, w.c., 665°C/12h, 620°C/40h	Kawasaki Steel Corp., Japan	485
22NiMoCr3-7	ANP-4	forging	890° C/4h, w.c., 650°C/7h, a.c.	Japan Steel Works, Japan	532
15Kh2MFAA	GW8	forging	1000°C, o.q., 680°C-720° C, a.c., 665°C/31-90h, c.f.	Škoda, Czech Republic	532

w.c., a.c., c.f., and o.q. denote water cooled, air cooled, cooled in furnace, and oil quenched, respectively

Code	C	Mn	Si	Cr	Ni	Mo	V	P	Cu
JFL	0.17	1.44	0.25	0.20	0.75	0.51	0.004	0.004	0.01
JRQ	0.18	1.42	0.24	0.12	0.84	0.51	0.002	0.017	0.14
JPB	0.20	1.42	0.26	0.15	0.83	0.54	0.01	0.017	0.01
JPC	0.18	1.45	0.27	0.15	0.81	0.54	0.01	0.007	0.01
ANP-4	0.21	0.85	0.22	0.39	0.84	0.55	-	0.006	0.05
GW8	0.15	0.45	0.30	2.86	0.1	0.79	0.30	0.008	0.048

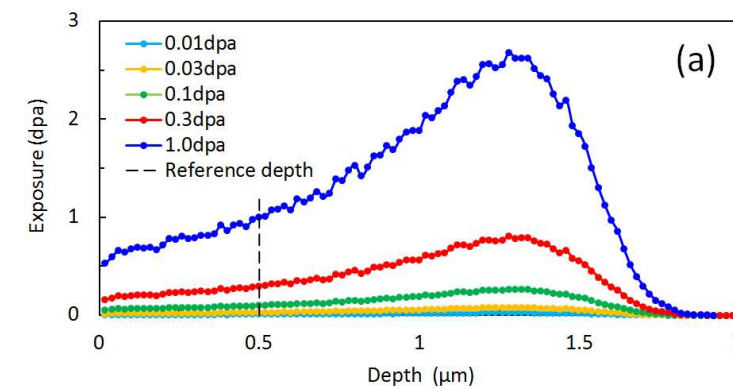
Composition of the considered RPV steels in wt % (balance Fe).

Ion-irradiation conditions and nanoindentation setup

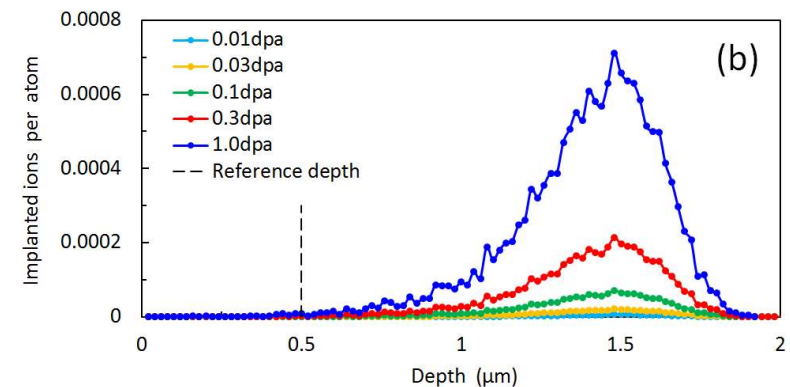
- IBC (Ion Beam Center) of HZDR
- Fe^{2+} , 5 MeV, 300° C
- Flux: $11^{11} \text{ ions/cm}^2/\text{s}^{-1}$
- Scan focused beam
- Normal incidence

Exposure (dpa)	Exposure (10^{14} cm^{-2})	Beam current (nA)	Irradiation time
0.01	0.27	70	8 min
0.03	0.80	130	13 min
0.1	2.66	100-120	1 h
0.3	7.98	130-140	2 h 20 min
1	26.6	120-160	8 h 30 min

- UNAT (Universal Nanomechanical Tester)
ASMEC GmbH, Berkovitch indenter
- Maximal load: $F_{\max} = 50 \text{ mN}$
- Indentation pattern of 6x6 indents separated by a spacing of $50 \mu\text{m}$
- Specimen size: $10 \times 10 \times 1 \text{ mm}$ size

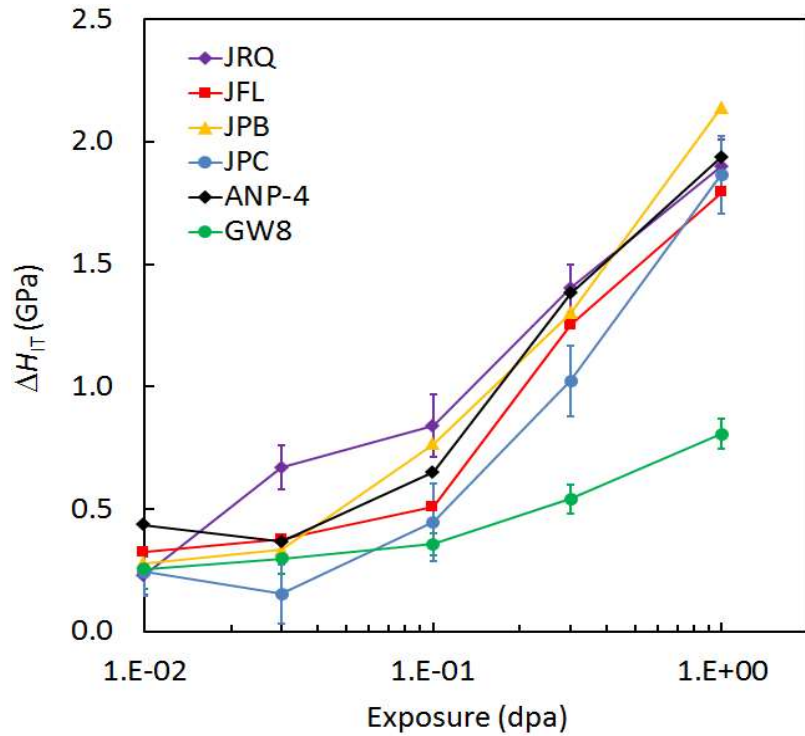


SRIM calculation



Implanted self-ions: $< 10^{-5} \text{ ions/atom}$ (1 dpa)

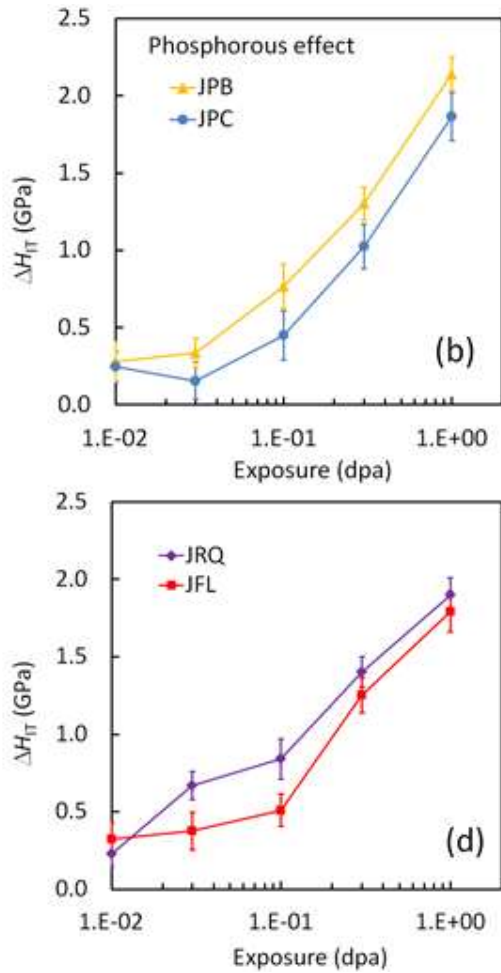
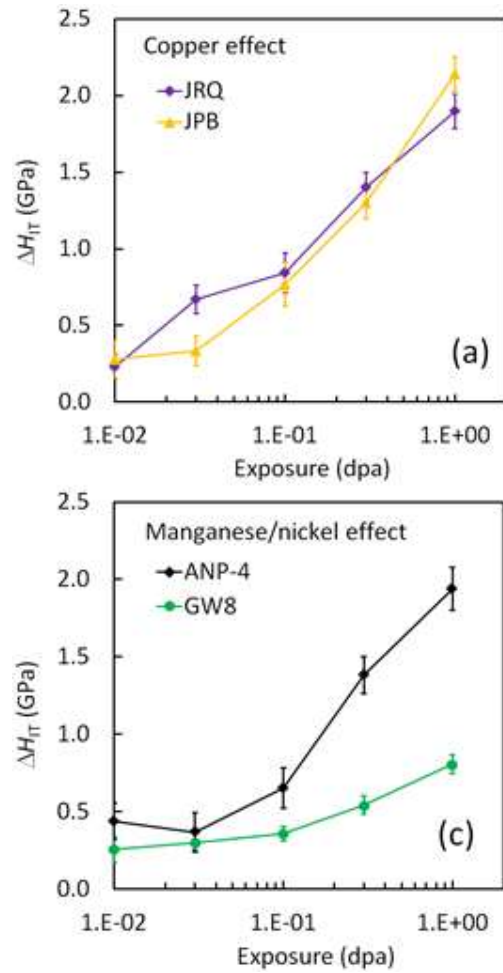
Hardness versus fluence



- Increasing dpa = growing hardness increase
- RPV steels of high Mn and Ni exhibit a stronger hardness increase
- Fit with a power-law exponent: 0.38-0.52 (exception: GW8: 0.25)

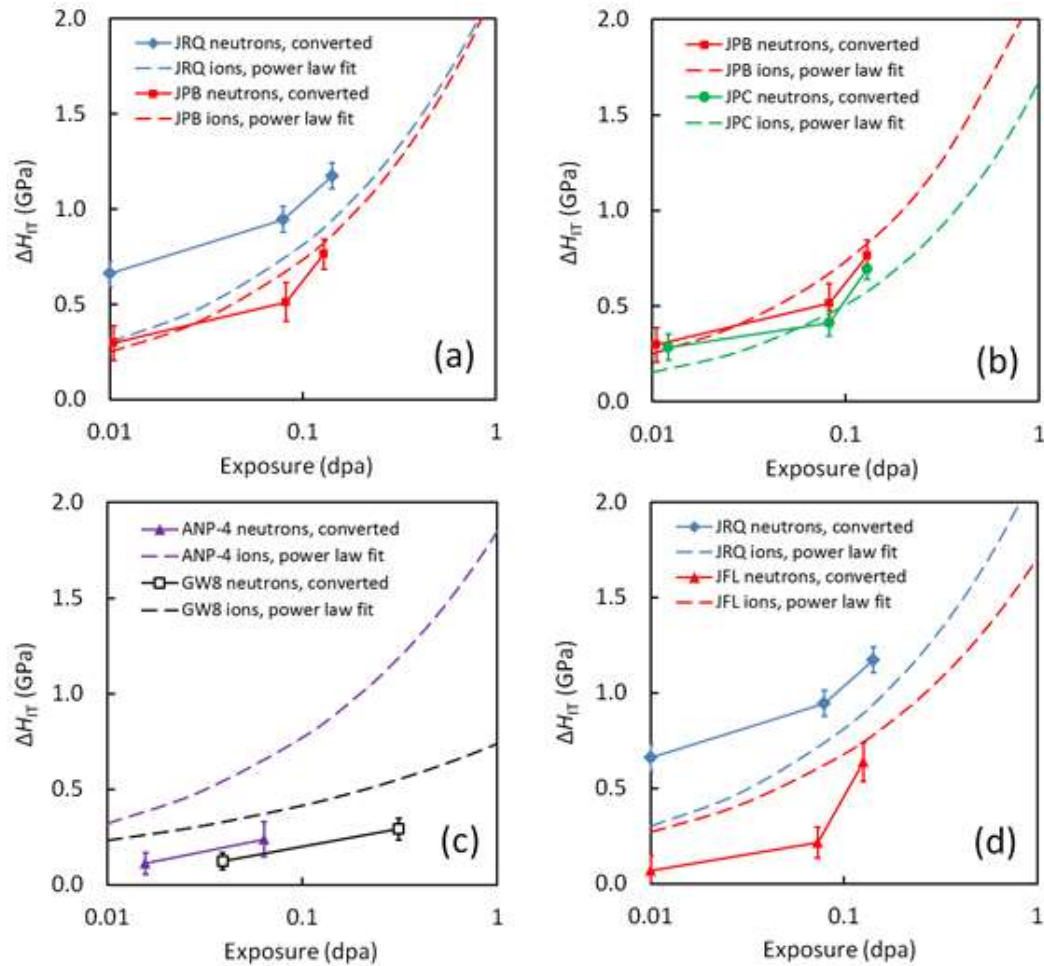
Hardness increase measured at a contact depth of 200 nm

Ion-irradiation induced hardening



- JRQ/JPB: Cu-rich clusters cannot pose the dominant contribution to hardening
- JPB/JPC: P effect on the hardening, stabilisation of cascade remnants by P?
- ANP4- GW8: Mn and/or Ni effect, Mn-enhanced loops formation ?
- JRQ/JFL: effect of P (instead of Cu)

Comparison with neutron irradiation-induced hardening



Transferability issues may exist:

- Dose rate effects
- Continuous neutron irradiation versus scanning ion beam
- Injected interstitial effects
- C contamination
- JRQ/JPB: Different contribution of Cu-rich-clusters to hardening (different radiation-induced nanofeatures ?)
- JPB/JPC: Ion irradiation seems to enhance the effect of P
- ANP4- GW8: Mn (and Ni) effect more pronounced for ions than for neutrons
- JRQ/JFL: Different contribution of Cu-rich clusters to hardening

Conclusions

- CEA contribution: Ion-irradiated Fe-3at.%Mn and Fe-3at.%Ni model alloys:
 - FeNi: RIS at high flux and RIP at low flux
 - FeMn: RIS (both fluxes)
 - Mn: more efficient dragging through vacancy and SIA; The enrichment is more important at PD sinks
- HZDR contribution: Nanoindentation test on a batch of ion-irradiated RPV steels
 - Difference between ion and neutrons irradiated steels
 - Different contribution of Cu-rich clusters to hardening (different radiation-induced nanofeatures ?)
 - Ion irradiation seems to enhance the effect of P contrary to neutron irradiation
 - Mn (and Ni) effect more pronounced for ions than for neutrons



**THANK YOU
FOR YOUR
ATTENTION**